Preparation of mullite bonded porous SiC ceramics by an infiltration method

Atanu Dey · Nijhuma Kayal · Omprakash Chakrabarti

Abstract A powder compact of α-SiC and α-Al$_2$O$_3$ was infiltrated with a liquid precursor of SiO$_2$, which on subsequent heat treatment at 1500 °C produced a mullite bonded porous SiC ceramics. Results showed that infiltration rate could be estimated by using weight gain measurements and theoretical analysis. The bond phase was composed of needle-shaped mullite which was observed to be grown from a siliceous melt formed during the process of oxide bonding. The porous SiC ceramics exhibited a density and porosity of 2 g cm^{-3} and 30 vol%, respectively, and also a pore size distribution in a range of 2–15 μm with an average pore size of 5 μm. No appreciable degradation of room temperature flexural strength (51 MPa) was observed at high temperatures (1100 °C).

Introduction

Porous SiC ceramics has been a focus of current research in the field of porous materials. Among the various applications of porous SiC ceramics, catalyst supports, hot gas filters, molten metal filters, gas burner media, thermal insulation materials, etc., have received considerable attentions. SiC ceramics has proven abilities to withstand high temperatures, thermal and mechanical stresses, and corrosive attacks in challenging atmospheres which make the material suitable for these applications. A major problem for processing of the material is the need of very high

sintering temperatures (~2000 °C). This is mainly because of the covalent nature of SiC. Oxides with low sintering temperatures are added in the starting powders and when oxides are sintered, SiC powders are bonded. One notable example is clay-bonded porous SiC ceramics. Hot gas filters made of this material have shown satisfactory endurance (~240 days of continuous operation) at ~800 °C in an oxidizing atmosphere [1]. Different methods of formation of oxide bond phases were reported. She et al. [2] developed an oxidation bonding technique in which a powder compact of SiC was heat treated in air to bind SiC particles by oxidation derived SiO$_2$ glass. Chung and Kim [3] prepared SiO$_2$-bonded porous SiC ceramics with spherical pores by sintering in air a compact of SiC powder and polymer microbeads. Porous SiC ceramics bonded by SiO$_2$ and mullite were prepared by heating in air, a powder compact of SiC, Al$_2$O$_3$ and graphite—the oxidation derived SiO$_2$ reacted with Al$_2$O$_3$ forming mullite [4]. Nearly similar attempt was made by Bardhan and Bhargava [5] who sintered a slip cast powder compact to produce mullite bonded porous SiC. These methods of producing porous SiC suffered from many shortcomings. Oxidation bonding was limited in the depth of zone which could be oxidized; it was not suitable for large scale production. Mechanical mixing of powders introduced flaws in the sintered product due to inhomogeneous mixing. Colloidal powder processing was time consuming and required careful control of suspension rheology. A method of avoiding these problems is infiltration with a liquid (solution, sol, or slurry) into green powder compacts; oxide bond phase can be introduced by infiltration with a liquid precursor that is converted to an inorganic phase during decomposition upon heating. Assuming the porosity of the starting compact is uniformly distributed, the addition of an oxide bond phase by this technique should result in uniformly distributed bond phase. This method has been

A. Dey · N. Kayal · O. Chakrabarti (✉)
Non-Oxide Ceramics and Composites Divisions, Central Glass and Ceramic Research Institute, Council of Scientific and Industrial Research, 196, Raja S. C. Mullick Road, Kolkata 700 032, India
e-mail: omprakash@cgcri.res.in

exploited in the production of a large variety of unique microstructure—graded, multi-phase, dense, etc [6, 7]. We have used an infiltration method for preparation of SiO₂-bonded porous SiC ceramics [8]. This study aims at investigating the oxide bonding process by an infiltration method to produce mullite bonded porous SiC ceramics. Investigation was done to identify the process parameters that controlled infiltration in the system in which SiO_2 was added to SiC/Al_2O_3 powder compacts to produce mullite bonded porous SiC ceramics. Effects of the processing parameters on the material and mechanical properties of the final ceramics were also studied.

Experimental

Commercially available α-SiC (Grindwell Norton Ltd., India; SiC 98.20%, free carbon 0.25%, SiO_2 0.50%, Fe_2O_3 0.04% w/w) and α-Al_2O_3 powders (Indian Aluminum Co. Ltd., India; Calcined Al HIM-30 Grade, >98%) were used in this work. Petroleum coke powder (Assam Carbon Products Ltd., India; ash content 0.68% w/w) was used as the pore forming agent. The SiC particles were of irregular shapes with non-uniform distribution of sizes. The d_{10}, d_{50}, and d_{90} of the SiC powder were found to be 9.48, 22.48, and 43.11 μm, respectively. The Al_2O_3 powder had distributed sizes with d_{10}, d_{50}, and d_{90} of 2.69, 6.49, and 13.08 μm, respectively. The petroleum coke powder had a BET surface area (NOVA 400 e, Quantachrome Instruments Inc., USA) of 4.87 m^2/g. SiC, Al_2O_3, and petroleum coke powders were weighed in a desired ratio (SiC:0.25Al_2O_3:0.13C), wet-mixed via ball milling in a suitable liquid medium for 18 h, dried in air to remove the solvent and finally oven dried at 100 °C. The powder mixture was mixed with 10% solution of polyvinyl alcohol (Loba Chemie, India; 10 wt% PVA in water), kneaded well to develop suitable workability and pressed at 23 MPa pressure in a stainless steel die. The pressed samples (rectangular bars of $50 \times 20 \times 16$ mm³) were dried in an air oven at 100 °C and dimensional measurements and weight were taken. The bars were subsequently fired at 1100 °C to burn off carbon; the dimensions and weight were again measured. Silica sol was prepared following acid hydrolysis of tetraethyl orthosilicate, TEOS, (Acros Organics, NJ, USA; purity 98%) and subsequent polycondensation reaction. The sol was stabilized at a pH of 1.6 and theoretically it contained SiO_2 of 21.88% w/w. A representative sample ($18 \times 20 \times 16$ mm³) was cut from the 1100 °C bar, dried, suspended in the silica sol by an wire attached to an electric balance (Metler PE 400, USA) and its weight was recorded as a function of time. In a separate experiment, well-dried 1100 °C bar samples were infiltrated with the silica sol, the infiltrated samples were dried to evaporate the solvent and the process was repeated. The

increase in mass relative to the initial weight was determined to assess the infiltration behavior under repetitive conditions. The infiltrated samples were fired at 1500 °C for 2 h in a chamber furnace (Electroheat, EN 170QT, Naskar & Co., West Bengal, India) with a programmed heating and cooling to yield porous SiC ceramics. The weight and dimensions of fired samples were measured. Density of the final ceramics was measured by water displacement method (Archimedes method) and porosity by boiling water method. Pore size distribution was measured by the Hg-intrusion porosimetry method (Poremaster, Quantachrome Instruments Inc., Florida, USA). The presence of crystalline phases were determined by XRD analysis (PW 1710, Philips, Holland, with Cu Kα radiation, $\lambda = 1.5406$ Å). Morphology and distribution of phases were examined by a scanning electron microscope (Model SE-440, Leo-Cambridge, Cambridge, UK). For mechanical property evaluation, the specimens were sliced to produce rectangular bars of cross section of 4.75 by 3.25 mm²; they were ground up to 10 μm finish and tensile surfaces were chamfered. The room temperature flexural strength was determined in three and four-point mode (with a span of 40 mm and cross-head speed of 0.5 mm/min) using an Instron Universal Testing machine. The deflection was monitored through LVDT with a resolution of 0.05% of full scale and from the load deflection data the Young's modulus was automatically obtained using standard software (Instron Bluehill-2, UK). The high temperature flexural strength was determined at 900 and 1100 °C in four-point mode (with a span of 40 mm) using a bending strength tester (Model no. 422S, Netzsch, Germany).

Results and discussion

Preparation of SiC/Al_2O_3 powder compact

After heat treatment of well-dried pressed bars at 1100 °C, the specimens were found to be strong without any sign of breakage of edges and corners and had good handling strength. The samples exhibited negligible dimensional change (0.2–0.6%); they also showed loss in weight (~8% w/w) due to burning of carbon powder and increase in porosity. We observed that % weight loss was less than the weight % of carbon powder present in the bar samples. Samples with no carbon powder were also fired in identical conditions; they showed a gain in weight of ~1.7%. Oxidation weight gain was the reasons for the % weight loss lower than the content of carbon. Characteristics of 1100 °C bar samples are presented in Table 1. Now, if pores are considered as inclusions randomly distributed in a volume and if the pores are assumed to be identical spheres, the minimum inclusion volume needed for

formation of a continuous network of pores is reported to be around 16–22% [9, 10]. It, therefore, appeared that all the pores present in the 1100 °C specimens were interconnected forming an open porous network. The formation of continuous porous network helped in unhindered and uniform infiltration of liquid into the compact.

Silica sol infiltration into SiC/Al₂O₃ powder compact

During initial infiltration experiments, surface cracks developed after drying of the infiltrated specimens. The cracking phenomenon could be avoided by heating the pressed bars at 1100 °C. Sintered necks formed between the touching particles prior to any precursor infiltration; the bars were strengthened eliminating the possibility of formation of surface cracks. Such phenomenon was also observed by other authors during infiltration experiments [11]. The infiltration weight gain was plotted against square root of time ($t^{1/2}$). Following a rapid infiltration, the initial linear region of the infiltration curve departed smoothly to another linear region. Representative infiltration results of the 1100 °C SiC/Al₂O₃ bar samples of different bulk densities are shown in Fig. 1. The weight gain (ΔW) in a given period corresponds to the amount of the liquid precursor infiltrated. If the bulk density of the powder compact changes, it causes a change in the void space available. For a particular composition of the powder compact, the void space is maximum at the minimum bulk density. The amount of liquid infiltrated will be maximum (W_1) at this maximum void space available. Then,

$$\text{Extent of infiltration} = (\Delta W/W_1) \times 100 \tag{1}$$

In case of SiC bars of same composition, but different densities, the ratio of extents of infiltration at a given point of time was the ratio of corresponding gains in infiltration weight obtained at that time. The ratio of the slopes of initial linear regions of the infiltration curves (at these densities) represented the ratio of the infiltration rates. Table 1 summarizes the infiltration rates (for the SiC bars of different characteristics) for the region where the rapid infiltration took place. Infiltration and flow of liquid through a porous solid have been well characterized and documented [11, 12]. According to these reports, infiltration is initially governed
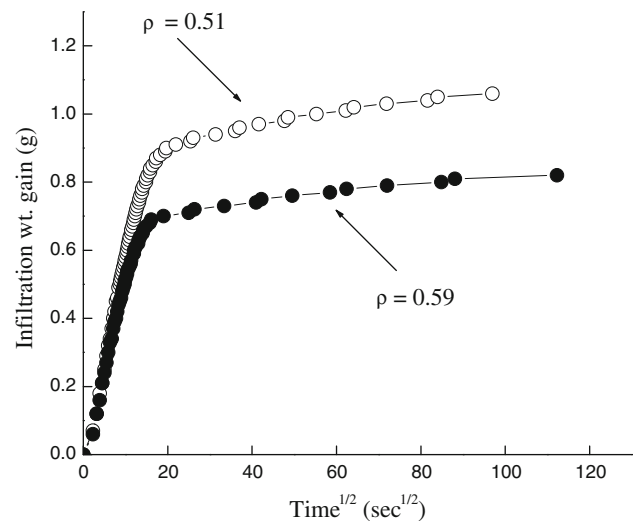

Fig. 1 Plot showing infiltration wt gain vs. (time)$^{1/2}$ for infiltration of a liquid precursor of silica into SiC/Al₂O₃ compacts having different relative densities

by a capillary force and the infiltration distance (h) at a given period (t) for a flow of liquid (of viscosity η, surface tension γ, and wetting angle θ) into a porous body (of relative density ρ and powder diameter D) can described by the Darcy's law: $h = [\{(2KP/\eta)\}t]^{1/2}$, where P ($= \{6\rho\gamma\cos\theta/D(1 - \rho)\}$) is the capillary pressure, K ($= D^2(1 - \rho)^3/36C\rho^2$) the permeability and C (~ 5, for cylindrical pore) the constant. The capillary infiltration behavior is parabolic in nature. In this study, linear infiltration curves were obtained at the initial stage which supported the capillary behavior of liquid flow. Capillary infiltration rates could be estimated by using the Darcy's law. The ratio of the theoretically calculated and experimentally measured infiltration rates for SiC bars of different characteristics showed good agreement (Table 1). In absence of any applied pressure, capillary pressure causes the wetting liquid to flow into the porous medium until the opposite pressure (P_a) of the compressed air becomes equal to the capillary pressure. In the later stage, compressed air can diffuse through the liquid and the infiltration distance at a given period can be described by the Fick's law: $h = \{(2D\beta P_a)t\}^{1/2}$, where β is the Henry's constant. In this study, parabolic nature of the diffusion of the compressed air

Table 1 Kinetic data for initial infiltration of liquid SiO₂ precursor into SiC and SiC/Al₂O₃ compacts having different bulk densities

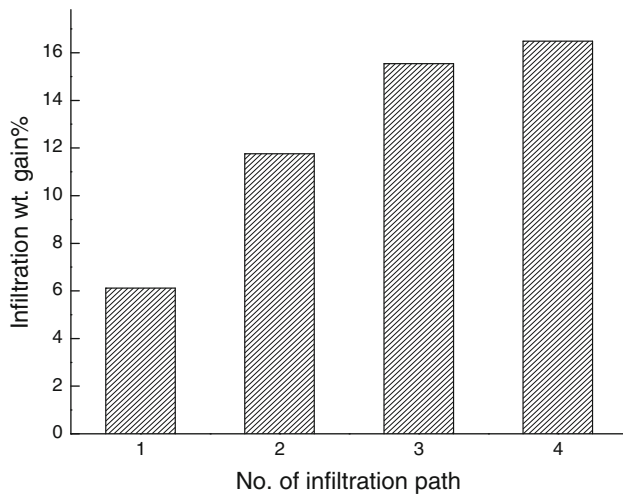| Type of 1100 °C bar	Bulk density (g cm⁻³)	Slope of infiltration weight gain vs. $t^{1/2}$ curve (g s$^{-1/2}$ × 10⁻²)	Ratio of experimentally measured capillary infiltration rates	Ratio of theoretically calculated (by using Darcy's law) capillary infiltration rates
SiC bar	1.70	6.49	1.25	1.30
	1.52	8.12		
SiC/Al₂0₃ bar	1.90	4.66	1.27	1.60
	1.63	5.92		

Fig. 2 Typical results showing effect of infiltration cycle on the amount of accumulated silica in a SiC/Al$_2$O$_3$ compact (of bulk density of 1.63 g cm^{-3})

through the liquid was also supported by the second linear regions of the infiltration curves.

Kinetic studies indicated that it was not possible to accumulate appreciable amount of silica into the 1100 °C specimen following a single pass infiltration run for a long period of time. Hence multi-pass infiltration was performed in order to load silica into the compact to a nearly constant level. During drying sol–gel silica accumulated into the porous channels resulting in gain in weight. Representative infiltration weight gain data for a SiC/Al$_2$O$_3$ bar of density of 1.63 g cm^{-3} are summarized in Fig. 2. As expected % mass increase due to silica accumulation was found to increase with number of infiltration pass. After third infiltration (15.94% w/w), the % mass increase recorded very small rise likely because of clogged pores. Thermal analysis showed that sol–gel silica transforms to crystalline silica (e.g., cristobalite) at ~1300 °C with 69.6% retention of initial weight [8]. An alumina/silica weight ratio of ~56/44 could be estimated using these values for the SiC/Al$_2$O$_3$ compact of density of 1.63 g cm^{-3}. This was indicative of a final composition lying in the mullite-aluminum silicate liquid phase field of stable Al$_2$O$_3$-silica

binary phase diagram [13]. This SiO$_2$-accumulated specimen was selected for subsequent oxide bonding study.

Formation of porous mullite bonded SiC ceramics

Material property and microstructure

After heat treatment at 1500 °C for 2 h, the SiO$_2$ accumulated specimen showed no change of shape, no sign of structural disintegration and crack formation; densification occurred with formation of a rigid porous body having a density of 2.02 g/cc and porosity of ~30 vol%. The process of densification was associated with negligible dimensional change (Table 2). Similar results of marginal to low shrinkages were also reported by other authors [5]. This indicates the net shape and net dimension formation capability of the oxide bonding process. The result of the XRD analysis of the porous ceramics is represented in Fig. 3. The ceramics was found to contain α-SiC, cristobalite, α-alumina, and mullite as major crystalline phases. The representative microstructure of the porous ceramic sample is shown in Fig. 4a. The densification behavior reflected formation of a liquid phase. Formation of a viscous phase was evident on the surface of the SiC particles; formation of necks was also observed in the contacting regions of the neighboring SiC particles in Fig. 4b. These necks could bridge the gap between the SiC particles. Pastila et al. [14] also viewed such well-developed necks connecting SiC particles in the microstructure of clay-bonded porous SiC ceramics. During microstructure examination, pores were seen to exist between SiC particles bonded by well-developed necks. The sizes of the pores were observed to be varying between 2 and 15 μm. Distribution of pore sizes was also determined by the Hg-intrusion porosimetry test (Fig. 5); the results indicated a variation of pore sizes within 2–10 μm and the average pore size was found to be 5.4 μm.

In the neck regions, mullite crystals formed were needle-shaped with rectangular faces (Fig. 6a, b). Such needle like crystalline growth was also noticed in stoichiometric mullite prepared using clay and reactive alumina [15]. The question arises as to how the presence of mullite can occur

Table 2 Characteristics of mullite bonded porous SiC ceramics

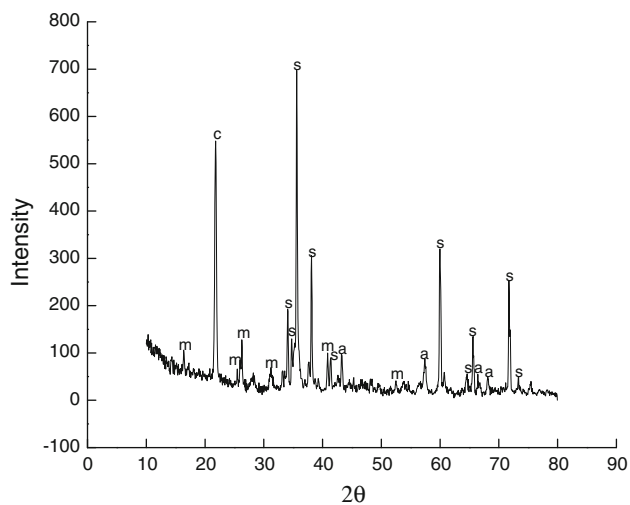| Dimensional changes			Bulk density (g/cc)	Porosity (%)	Mechanical property			
Length (%)	Width (%)	Thickness (%)			Young's modulus (GPa)	Flexural strength (MPa)[a]		
					Room temperature	Room temperature	900 °C	1100 °C
0.98	0.93	0.97	2.02	29.54	45.49 ± 3.82	46.98 ± 7.23	68.96 ± 11.89	58.24 ± 6.31

[a] Flexural strength was measured in 4-point bending mode

Fig. 3 XRD pattern of silica infiltrated SiC/Al$_2$O$_3$ compact heat treated at 1500 °C (*m* mullite, *c* cristobalite, *s* SiC, and *a* Al$_2$O$_3$)

Fig. 5 Pore size distribution profile of mullite bonded porous SiC ceramics determined by Hg-intrusion porosimetry method

in the final ceramics? Mullite can be prepared at low temperatures by using alumina and silica precursor materials. In amorphous single phase systems in which precursors were molecularly mixed, mullite crystallized at ∼1000 °C [16]. In diphasic mixtures (e.g., diphasic alumina–silica gels) prepared from colloidal boehmite (as the alumina source) and tetraethyl orthosilicate (as the silica source), alumina rich and silica rich precursors were segregated on a scale of ∼1–100 nm (average particle diameter of ∼20 nm) and mullite formation occurred at 1150–1350 °C [17, 18]. It was indicated that mullite formation occurred by nucleation and growth within the diphasic gel matrix. Growth of mullite proceeded preferentially through the siliceous phase. Investigation of mullitization kinetics of tailored diphasic aluminum silicate gels prepared by mixing fine particles of amorphous silica and boehmite, led Huling and Messing [19] to conclude
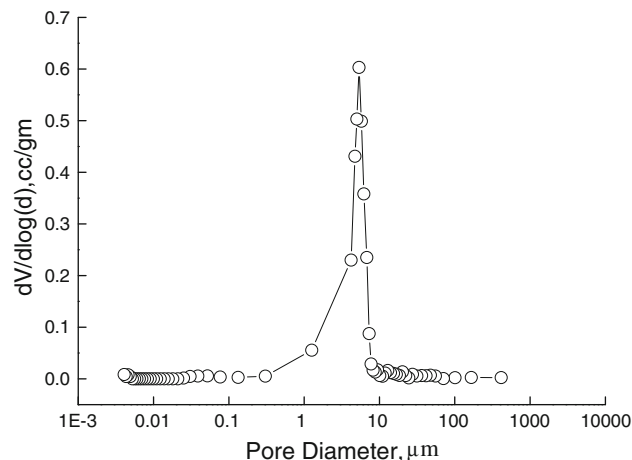
that the phase transformation was controlled by release of alumina into the siliceous phase (dissolution of alumina). Sundaresan and Aksay [20] provided several arguments that supported alumina dissolution as the rate controlling step for mullite growth in diphasic gels. Sacks et al. [21] observed alumina particles distributed in dense, continuous siliceous mixture in the microstructure of 1300 °C sintered compacts of micro-composite particles (consisted of ∼200 nm core of α-alumina particles (an order of magnitude larger than the typical alumina sources of the diphasic gels) and ∼15–20 nm coating of amorphous silica). Mullite formed at 1400–1425 °C and the authors also concluded that mullitization occurred primarily by nucleation as in diphasic gels. Rana et al. [22] detected mullite formation at 1415 °C in crystalline powder mixtures of alumina and silica (∼3 μm α-Al$_2$O$_3$ and quartz/cristobalite of same size). They suggested that a metastable eutectic reaction occurred at the alumina–silica interface forming a
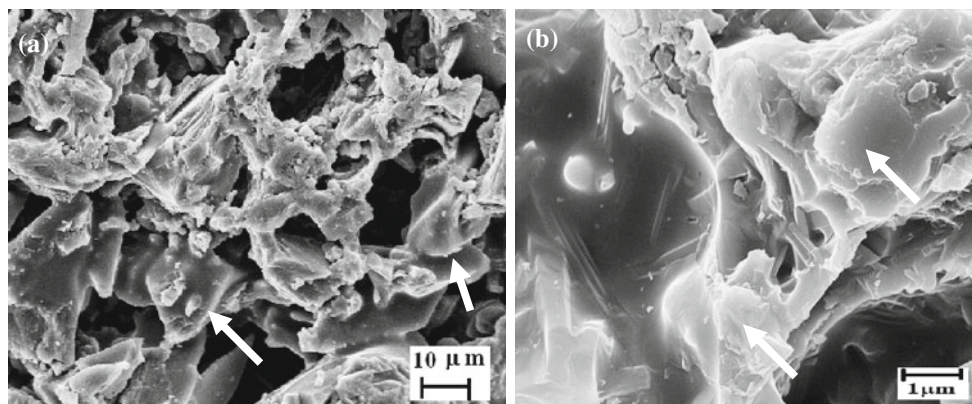

Fig. 4 SEM image of mullite bonded porous SiC ceramics. **a** presence of viscous phase on the surface of SiC particles bonded by oxides with formation of open porous network and **b** formation of

necks in the contacting regions of neighboring SiC particles (formation of viscous phase and neck is indicated by *arrows* in the figures)
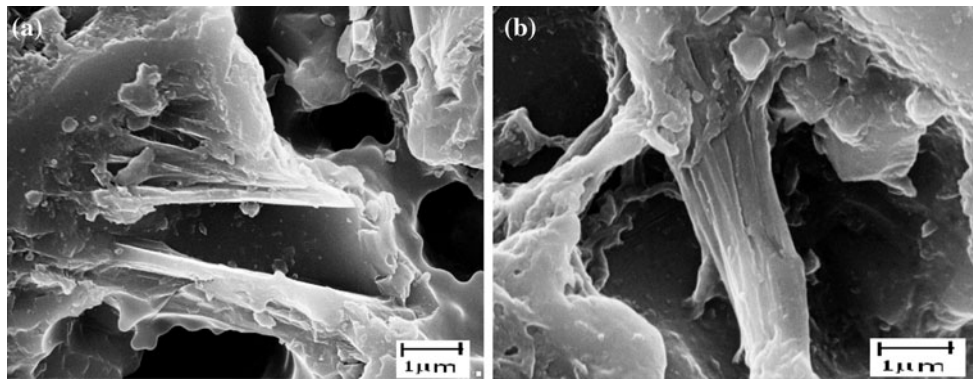
Fig. 6 SEM image showing the formation of needle-shaped mullite with rectangular faces in **a** the neck region and **b** in the bridge connecting neighboring SiC particles

liquid which was metastably saturated with alumina. If the solution reaction is faster, mullite keeps forming and does not grow. If the growth rate is faster, mullite is detected. Liquid formation reaction is associated with appreciable shrinkage and the mullite forming reaction involves expansion. All these studies involved alumina and silica source materials of varying sizes and types, but a liquid phase was a precursor to the formation of mullite in all these cases. Alumina and silica source materials of this study had some degree of similarity with those used by Sacks et al. A liquid phase appeared to have formed at any temperature below 1500 °C. Microstructure observations also indicated formation of a viscous phase. This study involved an overall composition of ~56 wt% alumina and ~44 wt% silica. The alumina particles were relatively coarser than those used in the mentioned studies. If mullite formation was controlled by alumina dissolution, a large amount of alumina needed to be dissolved in silica to attain the critical concentration for nucleation of mullite (~72 wt% alumina and ~28 wt% silica) and to maintain the necessary concentration for growth of mullite. This possibly hindered formation of mullite. Mullitization reaction was also not completed at 1500 °C, leaving residual alumina and silica in the final material. For completion of the mullitization reaction attainment of temperatures above 1500 °C (between 1550 and 1600 °C) was necessary [23]. Fineness of alumina particles would be another potential factor that controlled the completion of mullitization reaction. Therefore, the microstructural observations were consistent with the XRD results.

Mechanical property

The average values of Young's modulus and flexural strength of mullite bonded SiC porous ceramics are presented in Table 2. The 3-point (σ_{3pt}) and 4-point (σ_{4pt}) room temperature flexural strength values were found to be 51 and 46 MPa, respectively, giving a ratio of $\sigma_{3pt}:\sigma_{4pt} = 1.11$. The ratio was slightly lower than the value (1.24) obtained typically for ceramic materials [24]. No significant strength degradation was observed at temperatures of 900 and 1100 °C. An increase in strength was observed. Pastila et al. [14] also noticed increase in strength with increase in temperature in case of clay-bonded porous SiC ceramics. The room temperature mechanical properties are comparable with the values reported by other authors for similar materials. Ding et al. [4] obtained a room temperature flexural strength of ~24 MPa at a porosity level of ~44 vol%. The material synthesized by Bardhan and Bhargava [5] using a slip casting technique had a porosity of ~24 vol% and exhibited a room temperature flexural strength of ~63 MPa [5]. A higher sintering temperature (e.g., 1550 °C) was used in both these cases and consequently higher degree of mullitization appeared to have caused higher strength. Strength retention may indicate the suitability of the mullite bonded porous SiC ceramics for high temperature applications.

Conclusions

Synthesis of porous mullite bonded SiC ceramics was demonstrated by an infiltration technique consisting of intrusion of silica sol into powder compacts of SiC and Al_2O_3, followed by heat treatment at a temperature of 1500 °C in air. Infiltration of the liquid precursor of SiO_2 into SiC/Al_2O_3 powder compact occurred in two steps, viz., an initial rapid infiltration of the liquid governed by capillary pressure and a slow impregnation via diffusion of displaced air when the pressure of the entrapped air became equal to the capillary pressure. Parabolic rate laws were found to control both these steps. The number of infiltration passes regulated the amount of infiltrated silica. The final material was found to have porous structure formed by interconnected void spaces. The SiC particles were observed to be bonded by formation of necks at the

contacting points. Needle-shaped mullite was seen to have formed in the neck regions preferably through the formation of a siliceous liquid at temperatures below the heat treatment temperature of 1500 °C. Mullite bonded porous SiC material exhibited reasonable flexural strength values at room temperature and high temperatures at usable levels of porosity and pore sizes. Further improvement in mechanical property could be possible to be achieved by increasing the ceramization temperatures above 1500 °C and particle fineness of alumina with the completion of mullite bond phase formation and this particular aspect would be examined in future studies.

References

1. Okada S, Alvin MA (1998) Fuel Process Tech 56:143
2. She JH, Deng ZY, Doni JD, Ohji T (2002) J Mater Sci 37:3615. doi:10.1023/A:1016596805717
3. Chung YS, Kim YW (2005) Metal Mater Int 11:351
4. Ding S, Zeng YP, Jiang D (2008) Mater Charact 59:140
5. Bardhan N, Bhargava P (2008) Ceram Eng Sci Proc 29:127
6. Glass SJ, Green DJ (1988) Ceram Trans 1:784
7. Colvin PH, Lange FE (1996) J Am Ceram Soc 79:1810
8. Dey A, Kayal N, Chakrabarti OP (2011) Ceram Int 37:223
9. Zok F, Lange FF, Porter JR (1991) J Am Ceram Soc 74:1880
10. Lange FF, Atteraas L, Zok F, Porter JR (1991) Acta Metall Mater 39:209
11. Tu WC, Lange FF (1995) J Am Ceram Soc 78:3277
12. Constantz J, Herkelrath WN, Murphy F (1988) Soil Sci Soc Am J 52:10
13. Aksay IA, Pask JA (1975) J Am Ceram Soc 58:507
14. Pastila P, Nikkila AP, Mantyla T, Lara-Curzio E (2002) Ceram Eng Sci Proc 23:607
15. Viswabaskaran V, Gnanam FD, Balasubramanian M (2004) Appl Clay Sci 25:29
16. Li DX, Thomson WJ (1990) J Am Ceram Soc 73:964
17. Wei WC, Halloran JH (1988) J Am Ceram Soc 71:166
18. Li DX, Thomson WJ (1990) J Mater Res 5:1963
19. Huling JC, Messing GL (1991) J Am Ceram Soc 74:2374
20. Sundaresan S, Aksay IA (1991) J Am Ceram Soc 74:2388
21. Sacks MD, Bozkurt N, Scheiffele GW (1991) J Am Ceram Soc 74:2428
22. Rana APS, Aiko O, Pask JA (1982) Ceram Int 8:151
23. Sacks MD, Wang K, Scheiffele GW, Bozkurt N (1997) J Am Ceram Soc 80:663
24. Fischer J, Stawarczyk B, Hammerle CHF (2008) J Dent 36:316